

## Research Article

# Distributed Temporal Multiple Description Coding for Robust Video Transmission

Olivier Crave,<sup>1,2</sup> Christine Guillemot,<sup>1</sup> Béatrice Pesquet-Popescu,<sup>2</sup> and Christophe Tillier<sup>2</sup>

<sup>1</sup> *Institut de Recherche en Informatique et Systèmes Aléatoires, Institut National de Recherche en Informatique et en Automatique, 35042 Rennes Cedex, France*

<sup>2</sup> *Groupe des Écoles des Télécommunications, Département TSI Signal-Images, École Nationale Supérieure des Télécommunications, 46 rue Barrault, 75634 Paris Cédex 13, France*

Correspondence should be addressed to Olivier Crave, [olivier.crave@tsi.enst.fr](mailto:olivier.crave@tsi.enst.fr)

Received 22 March 2007; Accepted 6 June 2007

Recommended by Peter Schelkens

The problem of multimedia communications over best-effort networks is addressed here with *multiple description coding* (MDC) in a distributed framework. In this paper, we first compare four video MDC schemes based on different time splitting patterns and temporal two- or three-band motion-compensated temporal filtering (MCTF). Then, the latter schemes are extended with systematic lossy description coding where the original sequence is separated into two subsequences, one being coded as in the latter schemes, and the other being coded with a Wyner-Ziv (WZ) encoder. This amounts to having a systematic lossy Wyner-Ziv coding of every other frame of each description. This error control approach can be used as an alternative to automatic repeat request (ARQ) or forward error correction (FEC), that is, the additional bitstream can be systematically sent to the decoder or can be requested, as in ARQ. When used as an FEC mechanism, the amount of redundancy is mostly controlled by the quantization of the Wyner-Ziv data. In this context, this approach leads to satisfactory rate-distortion performance at the side decoders, however it suffers from high redundancy which penalizes the central description. To cope with this problem, the approach is then extended to the use of MCTF for the Wyner-Ziv frames, in which case only the low-frequency subbands are WZ-coded and sent in the descriptions.

Copyright © 2008 Olivier Crave et al. This is an open access article distributed under the Creative Commons Attribution License, which permits unrestricted use, distribution, and reproduction in any medium, provided the original work is properly cited.

## 1. INTRODUCTION

Due to the real-time nature of envisioned data streams, multimedia delivery usually makes use of transport protocols, that is, User Datagram Protocol (UDP) and/or Real-time Transport Protocol (RTP) which do not include control mechanisms which would guarantee a level of Quality of Service (QoS). The data transmitted may hence suffer from losses due to network failure or congestion. Traditional approaches to fight against losses mostly rely on the use of Automatic repeat request (ARQ) techniques and/or forward error correction (FEC). ARQ offers to the application level a guaranteed data transport service. However, the delay induced by the retransmission of lost packets may not be appropriate for multimedia applications with delay constraints. FEC consists in sending redundant information along with the original information. The advantage of FEC is that there is no need for a feedback channel. However, if the channel

degrades rapidly due to fading or shadowing, or if the estimated probability of transmission errors is lower than the actual value, then the FEC parity information is not sufficient for error correction. Hence, the video quality may degrade rapidly, leading to the undesirable *cliff* effect.

Multiple description coding (MDC) has been recently considered for robust video transmission over lossy channels. Several correlated coded representations of the signal are created and transmitted on multiple channels. The problem addressed is how to achieve the best average rate-distortion (RD) performance when all the channels work, subject to constraints on the average distortion when only a subset of channels is correctly received. Practical systems for generating descriptions that would best approach these theoretical bounds have also been designed considering the different components of compression system, as the spatio-temporal transform or the quantization. The reader is referred to [1] for a comprehensive general review of MDC.

Wyner-Ziv (WZ) coding can also be used as a forward error correction (FEC) mechanism. This idea has been initially suggested in [2] for analog transmission enhanced with WZ-encoded digital information. The analog version serves as side information (SI) to decode the output of the digital channel. This principle has been applied in [3, 4] to the problem of robust digital video transmission. The video sequence is first conventionally encoded, for example, using an MPEG coder. The resulting bitstream constitutes the systematic part of the transmitted information which could be protected with classical FEC. Errors in parts of the bitstream, for example, the temporal prediction residue in conventional predictive coding, may still lead to predictive mismatch and error propagation. The video sequence is in parallel WZ-encoded, and the corresponding data is transmitted to facilitate recovery from this predictive mismatch. The Wyner-Ziv data can be seen as extra coarser descriptions of the video sequence, which are redundant if there is no transmission error. The conventionally encoded stream is decoded and the corrupted data is reconstructed using error concealment techniques. The reconstructed signal is then used to generate the SI to decode the WZ-encoded data. However, error propagation in the MPEG-encoded stream may negatively impact the quality of the SI and degrade the RD performance of the system.

This problem is addressed here by structuring the data to be encoded into two descriptions. In the first scheme, odd and even frames are splitted between the two descriptions. Three levels of a motion-compensated Haar decomposition are then applied on the frames of each description. In the second scheme, the frames are first splitted into groups of two consecutive frames between the descriptions. Three levels of a motion-compensated Haar decomposition are then applied on each description. The third and fourth schemes resemble the first and second ones but are built upon a three-band (3B) Haar MCTF [5]. These schemes result in good central Rate-Distortion (RD) performances, but in high-PSNR-quality variation at the side decoders.

The tradeoff between the performance of the central and side decoders obviously depends on the amount of redundancy between the two descriptions. The quality of the signal reconstructed by the side decoders can be enhanced by systematic lossy encoding of the descriptions. The original sequence is separated into two subsequences, one being encoded as in the latter schemes, the other being Wyner-Ziv encoded. This amounts to having a systematic lossy Wyner-Ziv coding of every other frame of each description. This error control system can be used as an alternative to ARQ or FEC. The additional bitstream can be systematically sent to the decoder or can be requested, depending upon the existence of a return channel and/or the tolerance of the application to latency. The amount of redundancy added in each description is mostly controlled by the quantization of the Wyner-Ziv data. This first approach leads to satisfactory RD performance of side decoders, however suffers from high redundancy which penalizes the central description, when used as an FEC mechanism. To cope with this problem, the method is then extended to the use of motion-compensated temporal filtering for the Wyner-Ziv frames, in which case only the

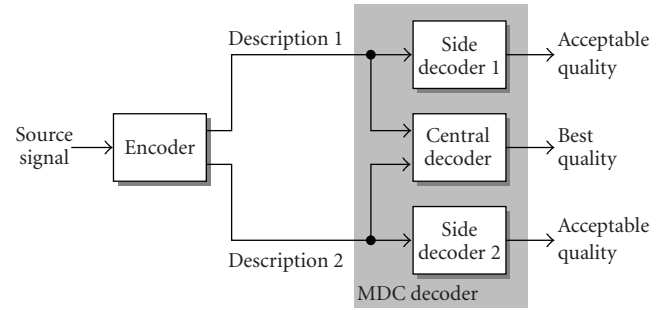


FIGURE 1: Generic MDC scheme with two descriptions.

low-frequency subbands are WZ-coded and sent in the descriptions.

The paper is organized as follows. Section 2 gives some background on MDC. Section 3 describes four video MDC schemes based on different time splitting patterns and temporal two- or three-band MCTF. Sections 4 and 5 show how some robustness can be added to these schemes using systematic lossy description coding. Section 6 reports the simulation results of the proposed codecs. Conclusions and perspectives are given in Section 7.

## 2. MULTIPLE DESCRIPTION CODING: BACKGROUND

In essence, MDC operates as illustrated in Figure 1. The MDC encoder produces several correlated—but independently decodable—bitstreams called *descriptions*. The multiple descriptions, each of which preferably has equivalent quality, are sent over as many independent channels to an MDC decoder consisting of a *central decoder* together with multiple *side decoders*. Each of the side decoders is able to decode its corresponding description independently of the other descriptions, producing a representation of the source with some level of minimally acceptable quality. On the other hand, the central decoder can jointly decode multiple descriptions to produce the best-quality reconstruction of the source. In the simplest scenario, the transmission channels are assumed to operate in a binary fashion; that is, if an error occurs in a given channel, that channel is considered damaged, and the entirety of the corresponding bitstream is considered unusable at the receiving end.

The success of an MDC technique hinges on path diversity, which balances network load and reduces the probability of congestion. Typically, some amount of redundancy must be introduced at the source level in order that an acceptable reconstruction can be achieved from any of the descriptions, and such that reconstruction quality is enhanced with every description received. An issue of concern is the amount of redundancy introduced by the MDC representation with respect to a single-description coding, since there exists a tradeoff between this redundancy and the resulting distortion. Therefore, a great deal of effort has been spent on analyzing the performance achievable with MDC ever since its beginnings [6, 7] until recently, for example, [8].

As an example of MDC, consider a wireless network in which a mobile receiver can benefit from multiple descriptions if they arrive independently, for example, on two neighboring access points. In this case, when moving between these two access points, the receiver might capture one or the other access point, and, in some cases, both. Another way to take advantage of MDC in a wireless environment is by using two frequency bands for transmitting the two descriptions. For example, a laptop may be equipped with two wireless cards (e.g., 802.11a and g) with each wireless card receiving a different description. Depending on the dynamic changes in the number of clients in each network, one wireless card may become overloaded, and the corresponding description may not be transmitted. In wired networks, different descriptions can be routed to a receiver through different paths by incorporating this information into the packet header [9]. In this situation, the initial scenario of binary “on/off” channels might no longer be of interest. For example, in a typical CIF-format video sequence, one frame might be encoded into several packets. In such cases, the system should be designed to take into consideration individual or bursty packet losses rather than a whole description. Several directions have been investigated for video using MDC. In [10–13], the proposed schemes are largely deployed in the spatial domain within hybrid video coders such as MPEG and H.264/AVC; a thorough survey on MDC for such hybrid coders can be found in [14].

On the other hand, only a few works investigated MDC schemes that introduce source redundancy in the temporal domain, although this approach has shown some promise. In [15], a balanced interframe MDC was proposed starting from the popular DPCM technique. In [16], the reported MDC scheme consists of temporal subsampling of the coded error samples by a factor of 2 so as to obtain two threads at the encoder which are further independently encoded using prediction loops that mimic the decoders (i.e., two-side prediction loops and a central prediction loop). MDC has also been applied to MCTF-based video coding: existing work for  $t + 2D$  video codecs with temporal redundancy addresses 3-band filter banks [17, 18]. Another direction for wavelet-based MDC video uses the polyphase approach in the temporal or spatio-temporal domain of coefficients [19–21].

### 3. TEMPORAL MULTIPLE DESCRIPTION CODING SCHEMES

Let us first consider the scheme illustrated in Figure 2 where odd and even frames are splitted between the two descriptions. One level of a motion-compensated Haar decomposition is then applied on the frames of each description. The temporal detail frames are encoded, while the passage from one level to the next one is done by interleaving the approximation frames from both descriptions. This new sequence will be subsequently distributed again among the two descriptions. This scheme will be called the Haar frame-level temporal MDC (F-TMDC) scheme.

The second scheme (see Figure 3), called the Haar GOF-level temporal MDC (G-TMDC) scheme, starts by splitting groups of two consecutive frames between the descriptions.

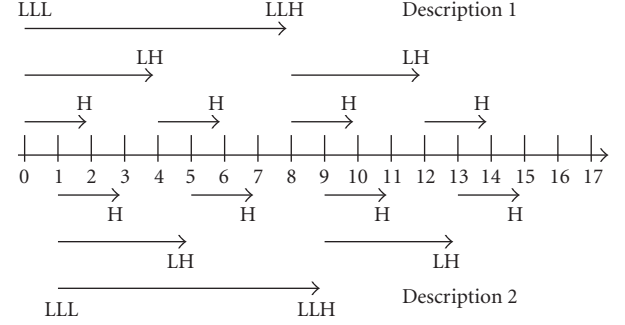


FIGURE 2: Haar F-TMDC: odd/even temporal splitting and two-band Haar MCTF.

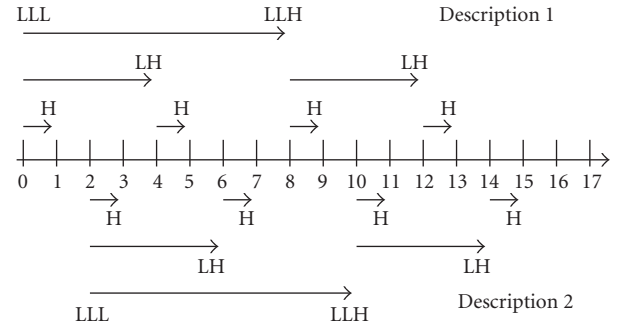


FIGURE 3: Haar G-TMDC: frames go two by two to descriptions and then a two-band Haar MCTF is applied in each one.

Again, one level of a Haar MCTF is applied to these couples of frames, and the details are encoded in their respective descriptions. As before, the passage from the first level to the next one is done by interleaving the approximation frames from the two descriptions. Next, the scheme continues as the Haar F-TMDC scheme, by encoding with Haar MCTF odd and even frames in different descriptions. One can remark that it is not possible to have the same gathering as at the first level in groups of two frames, since the temporal filtering would be performed on approximation frames coming from different descriptions, so in case one of them is lost, it will not be possible to reconstruct any of them. Another remark is that longer temporal filters would also be difficult to use in this framework, since for all the MDC schemes presented here, the temporal distance between frames in the same description is higher than one, and the longer the filter, the smaller the correlation between the frames. Therefore, we restrict ourselves to Haar MCTF, even though the coding performance of 5/3 MCTF is known to be better in absence of losses.

In this second scheme, since the encoding is performed on couples of successive frames, one can already expect a better performance of the central decoder of this scheme compared with the Haar F-TMDC scheme, where one over two frames is considered in each description. However, in the Haar F-TMDC scheme, when only one description is received, the side decoder will have to reconstruct one over two frames. The temporal distance between missing frames being only one, this task is not very difficult, and visual and

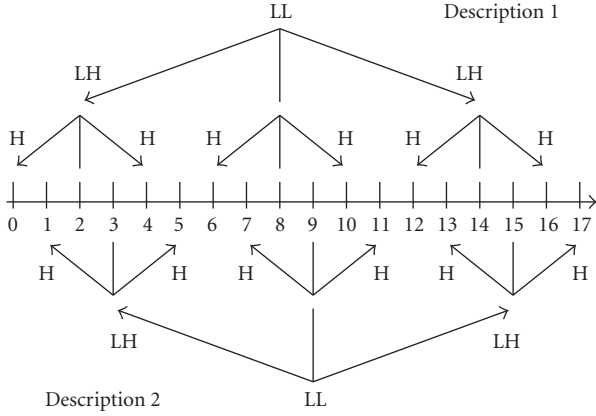


FIGURE 4: 3B F-TMDC: odd and even frames are separated and a 3-band MCTF is then applied in each description.

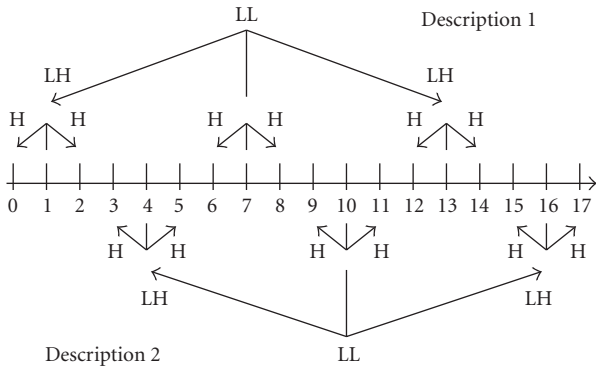


FIGURE 5: 3B G-TMDC: a 3-band MCTF is applied to groups of three frames of each description.

objective performance may be expected to be good. On the other hand, for the Haar G-TMDC scheme, the temporal distance between missing frames from the lost description is of two, so their interpolation could be more complex.

The third scheme, called the 3B F-TMDC scheme, illustrated in Figure 4 involves a temporal splitting of the input frames in odd and even ones, for the two descriptions, followed by a Haar 3-band MCTF on each flow, and approximation frames are interleaved to form the new sequence at the second decomposition level. Three-band Haar MCTF works like two-band Haar MCTF: a predict operator is applied in a symmetrical way between  $x_{3t}$  and  $x_{3t+1}$ , respectively, between  $x_{3t}$  and  $x_{3t-1}$ , resulting in two detail frames. Then, the update step involves the average of the motion-compensated details with the central frame  $x_{3t}$ . Improved update operators have been proposed for both two- and three-band schemes [22] minimizing the reconstruction error in these spatio-temporal filtering structures.

The last MDC scheme, called the 3B G-TMDC scheme, is similar to the 3B F-TMDC scheme, except that groups of three consecutive frames are separated in each description (see Figure 5). A Haar 3-band MCTF is applied this time on triplets. As in the case of two-band schemes, for this decomposition, compared with the previous one, one can expect

higher performance for the central decoder. At the side decoders, due to the greater temporal distance between frames used for interpolating missing ones, one may expect a deterioration compared to the 3B F-TMDC scheme. Indeed, for the 3B F-TMDC scheme, the temporal distance between missing frames is only one, while for the 3B G-TMDC scheme, the side decoders will have to interpolate from frames being spaced of three frames to fill in gaps resulting from the loss of one description. On the other hand, there is a gain in performance related to the fact that the original encoding is done on groups of consecutive frames, instead of frames spaced by one. These two antagonist trends will be studied in Section 6.

#### 4. SYSTEMATIC LOSSY DESCRIPTION CODING IN THE PIXEL DOMAIN

The schemes above present different tradeoffs between the quality (PSNR and visual) of the central and lateral descriptions. These tradeoffs depend on the amount of redundancy introduced in the two descriptions. In the MDC schemes above, the redundancy mostly results from the fact that, given the temporal splitting of the input sequence into two subsequences which form the descriptions, temporal correlation between adjacent frames in the input sequence is not optimally exploited. The quality of the signal reconstructed by the side decoders can be enhanced by systematic lossy encoding of the descriptions. In this section and in the simulation results, we only consider the 3B F-TMDC (Figure 4) and 3B G-TMDC (Figure 5) schemes of Section 3 but the Haar F-TMDC and G-TMDC schemes can be extended in a similar manner.

Let us first consider the MDC coding architecture depicted in Figure 6 (encoder) and Figure 7 (decoder). At the encoder, the source is first divided into two sequences leading to two *nonredundant* descriptions of the input sequence. Two approaches are considered for splitting the frames. In the first one, similarly to the 3B F-TMDC scheme of the previous section, the two subsequences are constructed by splitting odd from even frames as shown in Figure 8, while the second approach consists in separating the frames in groups of three frames as shown in Figure 9 as in the 3B G-TMDC scheme. The corresponding schemes will be referred to as 3B frame-level distributed MDC (F-DMDC) and 3B G-DMDC schemes. In each description, the frames of one subsequence are considered as *key frames* while the frames of the other are considered as Wyner-Ziv frames. The subsequence of key frames is first temporally transformed using a Haar 3-band MCTF with two levels of temporal decomposition. The remaining frames (Wyner-Ziv frames) are transformed with an integer  $4 \times 4$  block-based discrete cosine transform (DCT) and quantized with a uniform scalar quantizer. The transformed coefficients are structured into spatial subbands and each bit-plane of the quantized subbands is then separately turbo-encoded. The resulting parity bits are stored in a buffer. At the side decoders, the key frames are decompressed and the SI is generated by interpolating the intermediate frames from the key frames. The turbo decoder then corrects this SI using the parity bits. The parity sequences stored in the buffer are transmitted in small amounts upon decoder

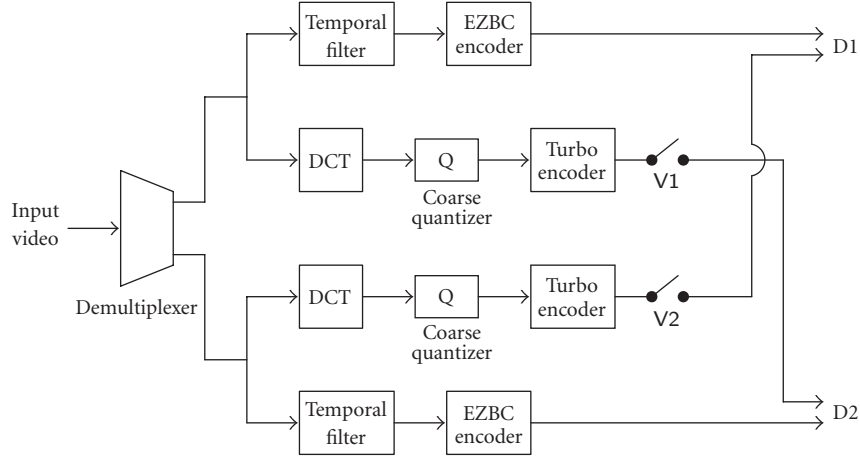


FIGURE 6: Implementation of the systematic lossy description encoder in the pixel domain.

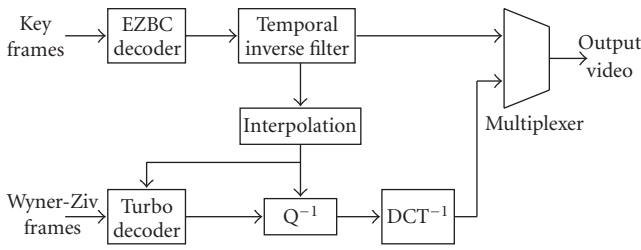


FIGURE 7: Implementation of the systematic lossy description side decoder in the pixel domain.

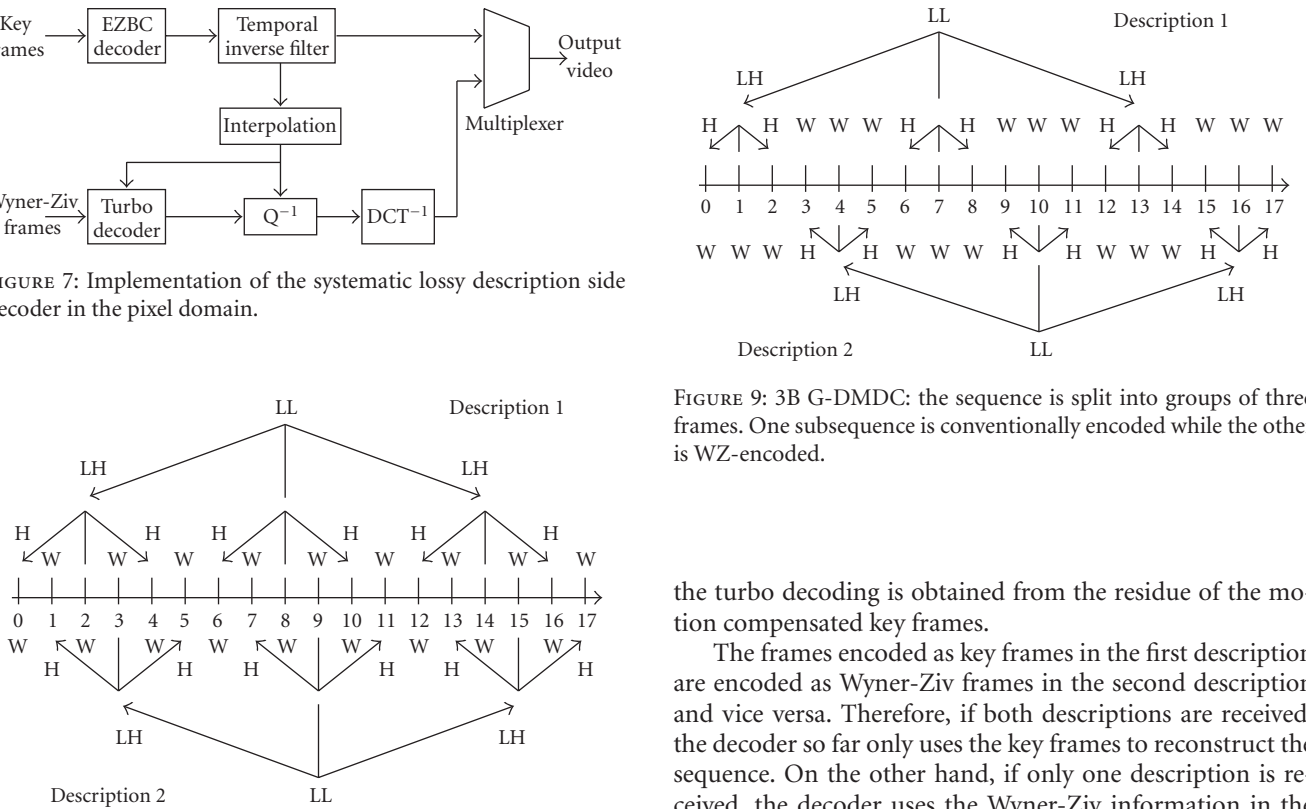


FIGURE 8: 3B F-DMDC: the sequence is split into its even and odd frames. One subsequence is conventionally encoded while the other is WZ-encoded.

request via the feedback channel. When the estimate of the bit error rate at the output of the decoder exceeds a given threshold, extra parity bits are requested. This amounts to controlling the rate of the code by selecting different puncturing patterns at the output of the turbo code. The bit error rate is estimated from the log likelihood ratio on the output bits of the turbo decoder. The correlation parameter used in

FIGURE 9: 3B G-DMDC: the sequence is split into groups of three frames. One subsequence is conventionally encoded while the other is WZ-encoded.

the turbo decoding is obtained from the residue of the motion compensated key frames.

The frames encoded as key frames in the first description are encoded as Wyner-Ziv frames in the second description and vice versa. Therefore, if both descriptions are received, the decoder so far only uses the key frames to reconstruct the sequence. On the other hand, if only one description is received, the decoder uses the Wyner-Ziv information in the received description to reconstruct the missing frames. The amount of redundancy is defined by the quantization of the Wyner-Ziv frames: the coarser the quantization, the higher the Wyner-Ziv bitrate. So far, when the scheme is used in an FEC scenario, the Wyner-Ziv streams are systematically sent and discarded at the central decoder. Further work will be dedicated to a possible use of the Wyner-Ziv bits even when both descriptions are received in order to improve the quality of the central decoder. In the ARQ scenario, the Wyner-Ziv streams are only sent if requested by the decoder. In the results reported later on, only the FEC scenario is considered.

It is important to notice that the Wyner-Ziv bitrate not only depends on the degree of quantization of the Wyner-Ziv



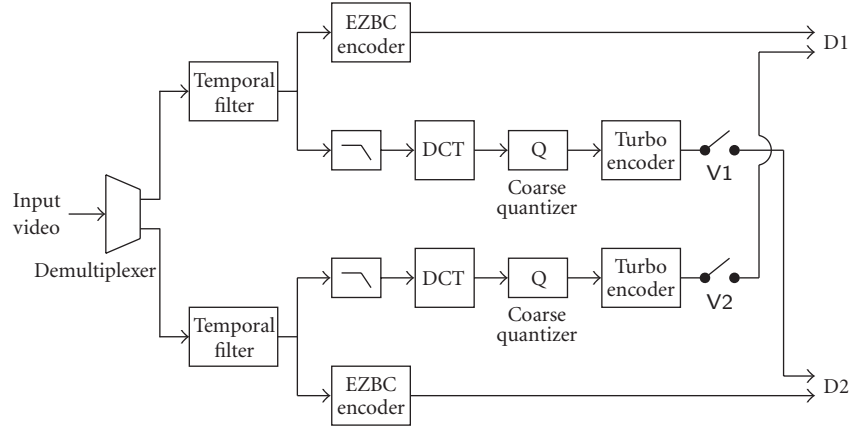


FIGURE 10: Implementation of the systematic lossy description encoder in the MCTF domain.

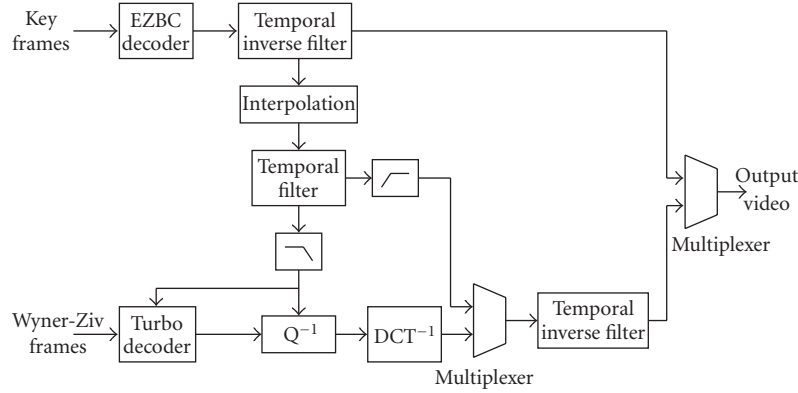


FIGURE 11: Implementation of the systematic lossy description side decoder in the MCTF domain.

frames, but also on the quality of the SI, and therefore on the degree of quantization of the key frames.

## 5. SYSTEMATIC LOSSY DESCRIPTION CODING IN THE MCTF DOMAIN

To reduce the Wyner-Ziv bitrate and improve the RD performance of the central decoder, a second architecture is proposed where the Wyner-Ziv frames are first transformed by the same Haar 3-band MCTF as the one used for the key frames in the 3B G-TMDC scheme but with only one temporal level to keep a reasonable distance between the subbands. Furthermore, before entering the Wyner-Ziv encoder, the subbands are lowpass-filtered such that only the low-frequency subbands are WZ-encoded. The codec architecture is depicted in Figures 10 (encoder) and 11 (decoder). For this codec, the approach of separating the frames according to the GOP size of the temporal filter is used to obtain the two subsequences as shown in Figure 12. At the side decoders, the SI is obtained by transforming the interpolated frames with a Haar 3-band MCTF and the resulting low frequencies are used as SI to decode the Wyner-Ziv subbands. To reconstruct the frames, the decoded low-frequency subbands are combined with the high-frequency subbands of the interpolated

frames to get a sequence of subbands that is finally inverse filtered and reconstructed.

We will see in Section 6 that since only the low frequencies are WZ-encoded, the RD performances at the central decoder should outperform the performances of the schemes presented in the previous section.

## 6. SIMULATION RESULTS

### 6.1. Performance analysis of the temporal MDC schemes

We first compare the four proposed MDC video coding schemes of Section 3. They have been implemented using the MC-EZBC software [23]. Three temporal levels of decomposition are performed for the two-band MCTF schemes (i.e., the Haar F-TMDC and Haar G-TMDC schemes) and two levels for the 3-band MCTF schemes (i.e., the 3B F-TMDC and 3B G-TMDC schemes). The MCTF is performed using hierarchical variable-size block matching (HVSBM) algorithm with block sizes varying from  $64 \times 64$  to  $4 \times 4$  and a 1/8th pel accuracy. Simulations have been conducted on several test sequences, and results are presented for Foreman and Hall Monitor, in QCIF format at 15 fps.

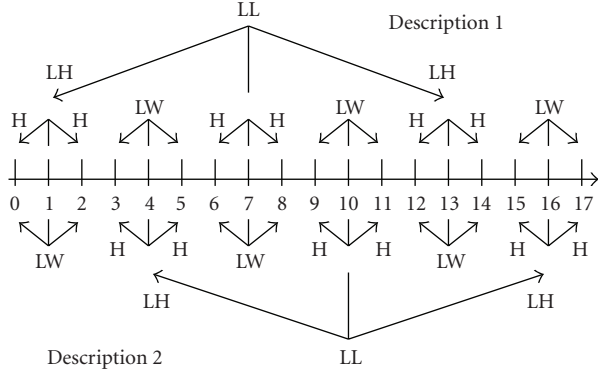


FIGURE 12: 3B G-DMDC scheme in the MCTF domain: the sequence is split into groups of three frames. One subsequence is conventionally encoded while the other is temporally filtered and only the low-frequency subbands are WZ-encoded.

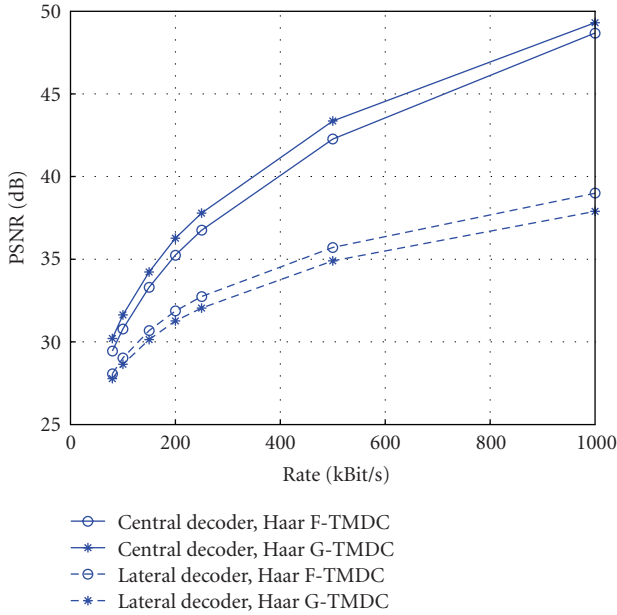


FIGURE 13: Performance comparison of the Haar F-TMDC and Haar G-TMDC schemes (Foreman, QCIF 15 fps).

The central and side RD performances of the Haar F-TMDC and Haar G-TMDC schemes, involving two-band MCTF, are shown in Figures 13 and 14. As expected, the central decoder of the Haar G-TMDC scheme performs better than that of the Haar F-TMDC scheme. The side decoder of the Haar F-TMDC scheme slightly outperforms the one of the Haar G-TMDC scheme. This reflects the difficulty of interpolating two consecutive frames when only one description is received in the Haar G-TMDC scheme. For the Foreman sequence, one can also remark that even though the two schemes only differ at the first temporal level of decomposition, the gap between their coding performances is quite large (around 2 dB and 1 dB for the central and side decoders, resp.). The performance gap is lower for the Hall Monitor se-

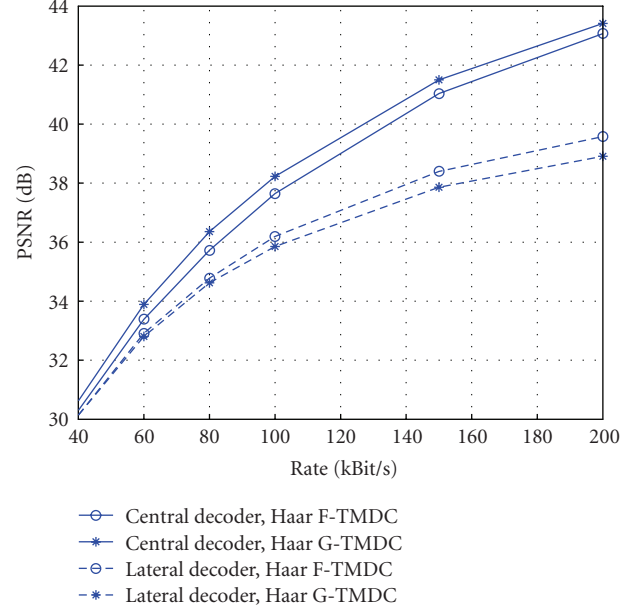


FIGURE 14: Performance comparison of the Haar F-TMDC and Haar G-TMDC schemes (Hall Monitor, QCIF 15 fps).

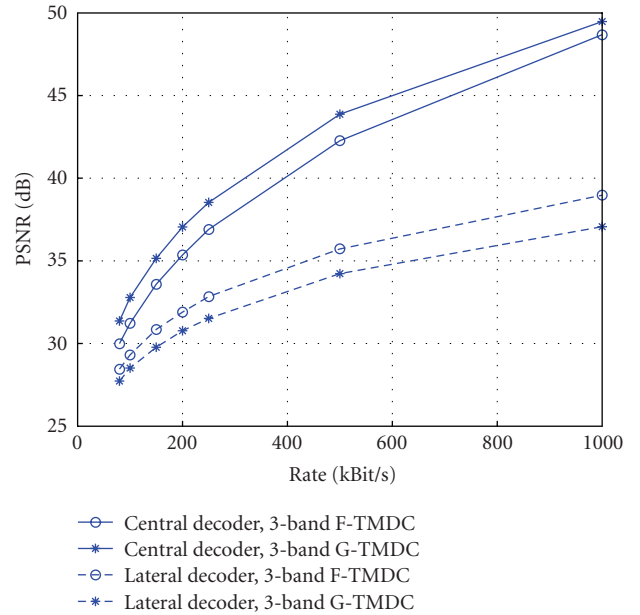


FIGURE 15: Performance comparison of the 3B F-TMDC and 3B G-TMDC schemes (Foreman, QCIF 15 fps).

quence (0.5 dB for the central decoders and only 0.25 dB for the side decoders).

The RD performance of the 3B F-TMDC and 3B G-TMDC schemes, based on 3-band MCTF, is illustrated in Figures 15 and 16. As in the case of two-band MCTF schemes, grouping consecutive frames before filtering and encoding them in different descriptions leads, as expected, to better results for the central decoder of the 3B G-TMDC scheme. An improvement of up to 1.5 dB for the Foreman

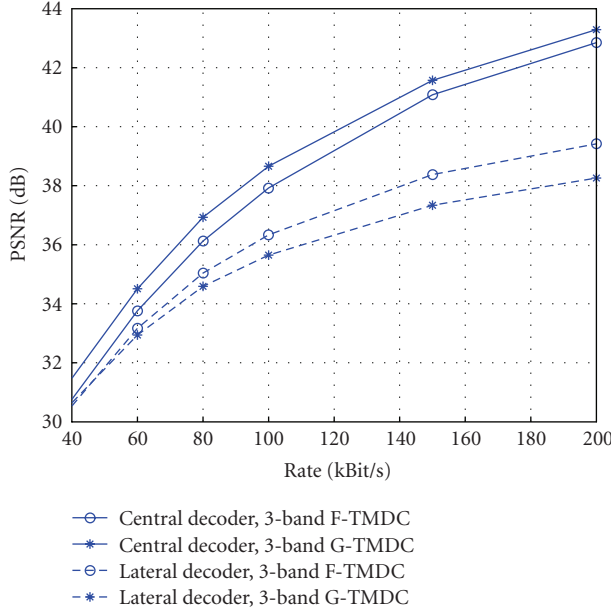


FIGURE 16: Performance comparison of the 3B F-TMDC and 3B G-TMDC schemes (Hall Monitor, QCIF 15 fps).

sequence and 0.5 dB for Hall Monitor has been obtained. This improvement is however obtained at the expense of a PSNR loss (of up to 2 dB for Foreman and 1 dB for Hall Monitor) of the side decoders. The side decoders need to interpolate three missing frames from frames which are temporally distant.

## 6.2. Performance analysis of the distributed MDC schemes

The PSNR and visual performance advantage brought by the Wyner-Ziv encoded data is then assessed. The results of the 3B F-DMDC and G-DMDC schemes are thus compared against the performance of the 3B MDC scheme [18]; it is based on the same 3-band MCTF but with temporal redundancy added by subsampling the temporal 3-band structure by a factor 2, instead of a factor 3.

The tests have been performed for four rate-distortion points for the Wyner-Ziv bitrate corresponding to the  $4 \times 4$  quantization matrices depicted in Figure 17. Within a  $4 \times 4$  quantization matrix, the value at position  $k$  in Figure 17 indicates the number of quantization levels associated to the DCT coefficients band  $b_k$ ; the value 0 means that no Wyner-Ziv bits are transmitted for the corresponding band. In the following, the various matrices will be referred to as  $Q_i$  with  $i = 1, \dots, 4$ . The higher the index  $i$ , the higher the bitrate and the quality.

The bitrates used for the key frames are 20, 40, 60, 80, 100, 150, and 200 kBit/s for Hall Monitor and 80, 100, 150, 200, 250, 500, and 1000 kBit/s for Foreman. Figures 18 and 19 show the performances of the 3B F-DMDC scheme at the central decoder for Foreman and Hall Monitor. The bitrate corresponds to the global rate (both descriptions). For Hall Monitor, the 3B F-TMDC scheme systematically out-

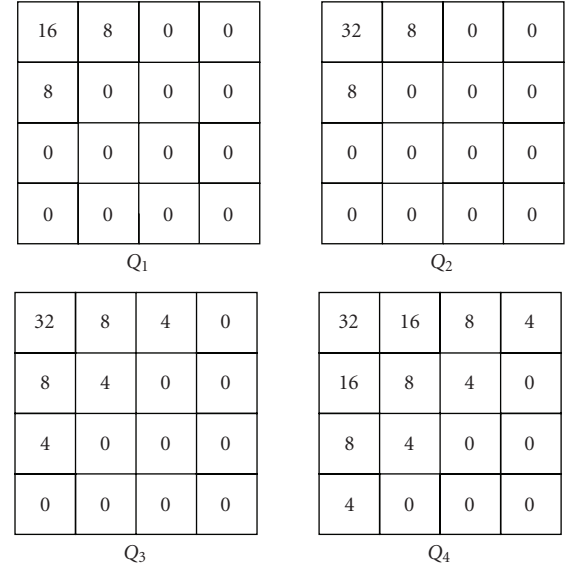


FIGURE 17: Four quantization matrices associated to different RD performances.

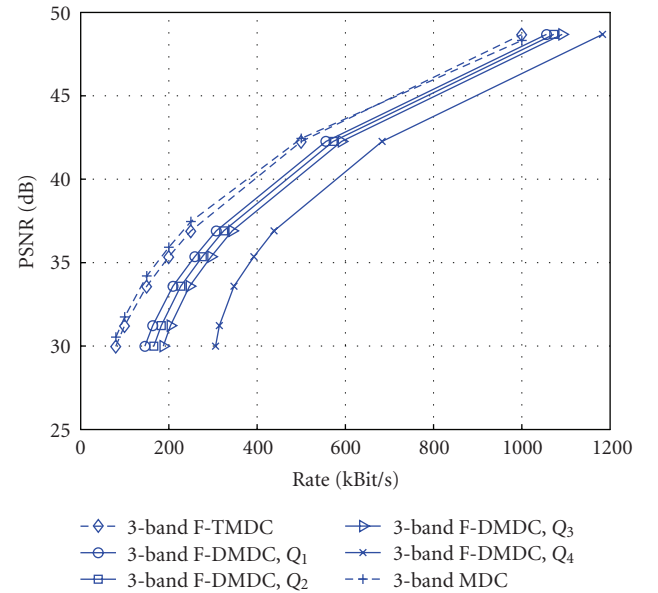


FIGURE 18: Central distortions of the 3B F-DMDC scheme compared with the 3B MDC codec (Foreman, QCIF 15 fps).

performs the 3B MDC scheme (+1 dB) but performs worse (−0.5 dB) in the case of Foreman. As expected, when a Wyner-Ziv stream is added to the descriptions, the PSNR values decrease. Figures 20 and 21 show the performances of the 3B F-DMDC scheme at the side decoder. This time, the 3B F-DMDC scheme slightly outperforms the 3B MDC scheme with or without extra information, especially for Foreman and for the highest bitrates.

A comparison of the schemes only in terms of mean PSNR (the average PSNR between the frames being received and the frames being lost and interpolated with or without extra information) is not sufficient because the PSNR fluc-



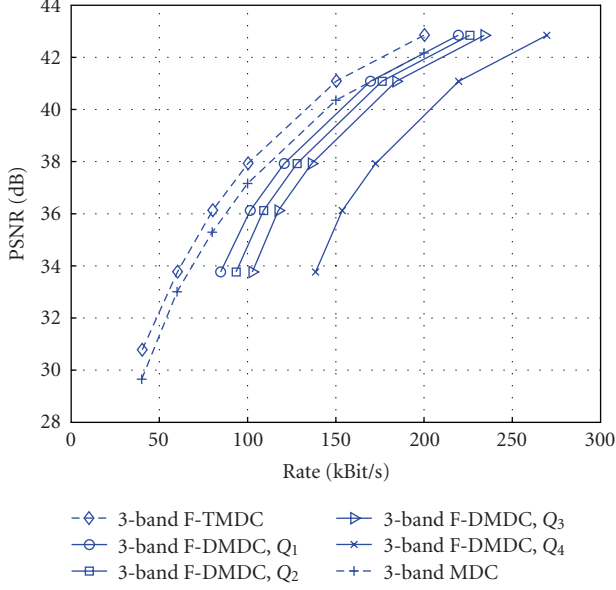


FIGURE 19: Central distortions of the 3B F-DMDC scheme compared with the 3B MDC codec (Hall Monitor, QCIF 15 fps).

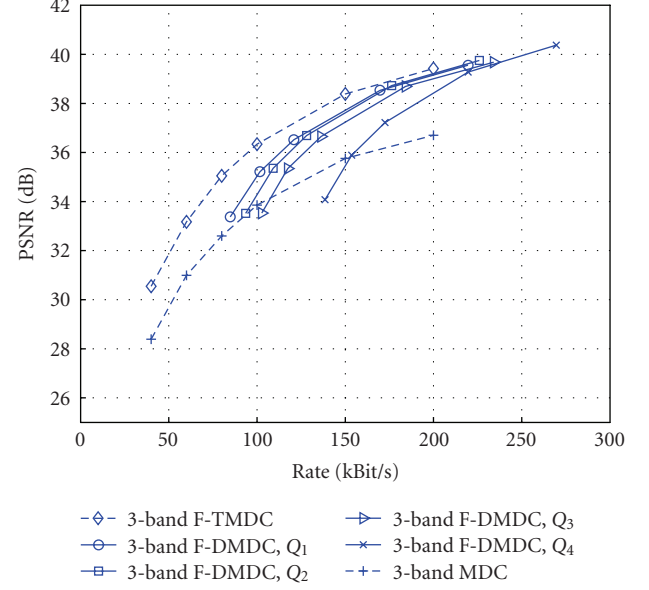


FIGURE 21: Side distortions of the 3B F-DMDC scheme compared with the 3B MDC codec (Hall Monitor, QCIF 15 fps).

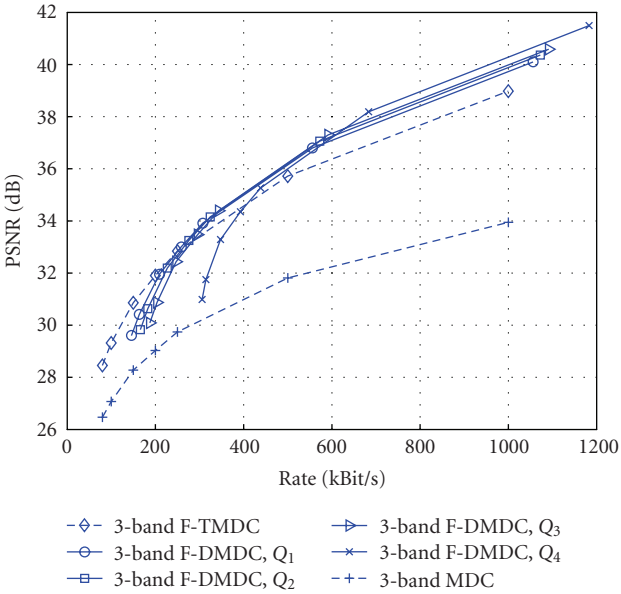


FIGURE 20: Side distortions of the 3B F-DMDC scheme compared with the 3B MDC codec (Foreman, QCIF 15 fps).

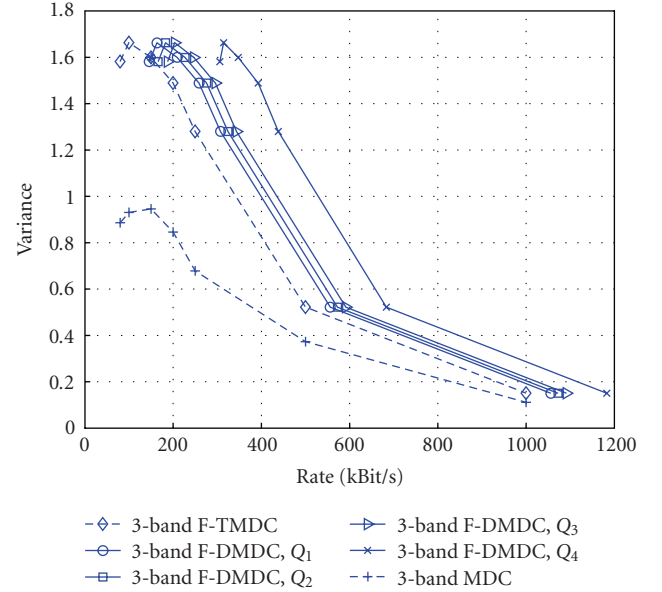


FIGURE 22: PSNR variations at the central decoder of the 3B F-DMDC scheme in the MCTF domain compared with the 3B MDC codec (Foreman, QCIF 15 fps).

tuations in time are not taken into account. Figure 24 shows the PSNR variation from the 50th to the 100th frame of the Foreman sequence at 307 kBit/s for the 3B F-DMDC scheme using the quantization matrix  $Q_1$  and the 3B MDC scheme at the central and side decoders. At the side decoder, this figure shows that the PSNR values of the 3B MDC scheme drop sharply (as low as 16.5 dB) when the missing frames are simply interpolated, whereas it is more stable for the 3B F-DMDC scheme (the lowest value being 25.9 dB), even though the mean PSNR value is only 1 dB lower for the 3B

MDC scheme than for the 3B F-DMDC scheme. However, at the central decoder, the 3B MDC scheme performs better than the 3B F-DMDC scheme (+2.2 dB) because the data contained in the Wyner-Ziv bitstream is simply discarded and does not contribute to the central decoding.

Figures 22 and 23 show the variations in PSNR between the frames at the central and side decoders. At the central decoder, the variance is higher for the F-DMDC scheme than for the 3-band F-TMDC and 3-band MDC schemes but remains reasonable (less than 1.8). At the side decoders, the

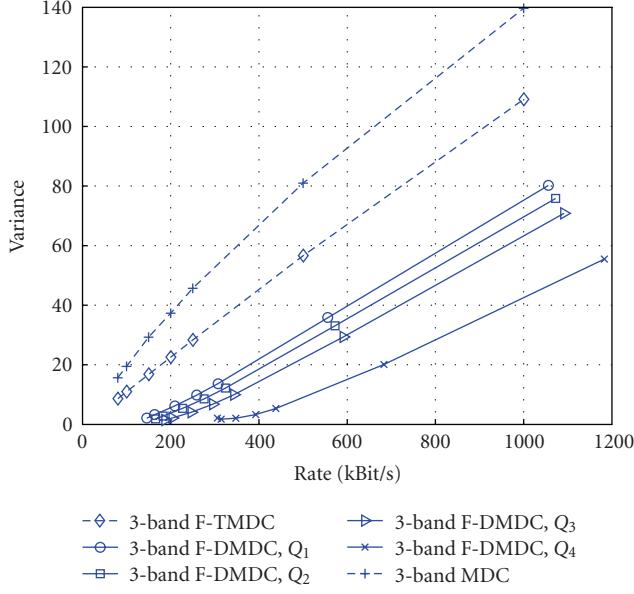


FIGURE 23: PSNR variations at the side decoder of the 3B F-DMDC scheme compared with the 3B MDC codec (Foreman, QCIF 15 fps).

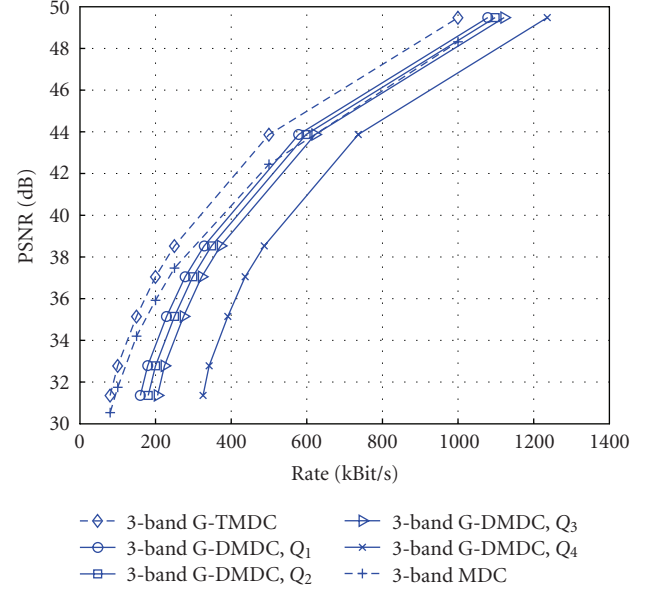


FIGURE 25: Central distortions of the 3B G-DMDC scheme compared with the 3B MDC codec (Foreman, QCIF 15 fps).

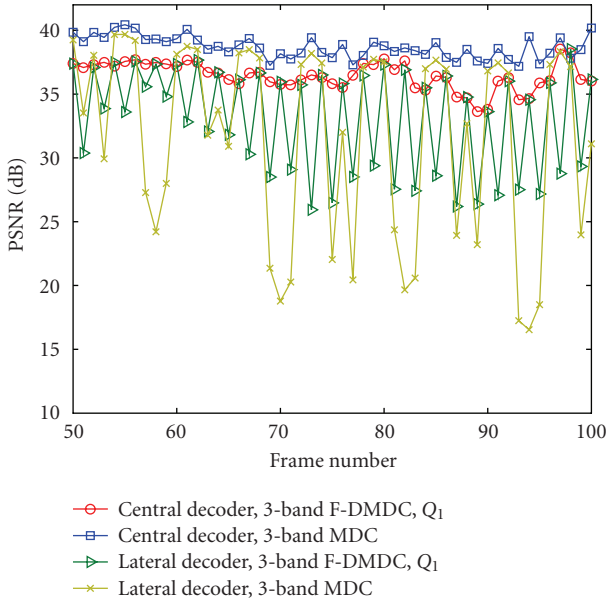


FIGURE 24: Central and lateral PSNR variation from the 50th to the 100th frame of the Foreman sequence (QCIF, 15 fps) at 307 kBit/s.

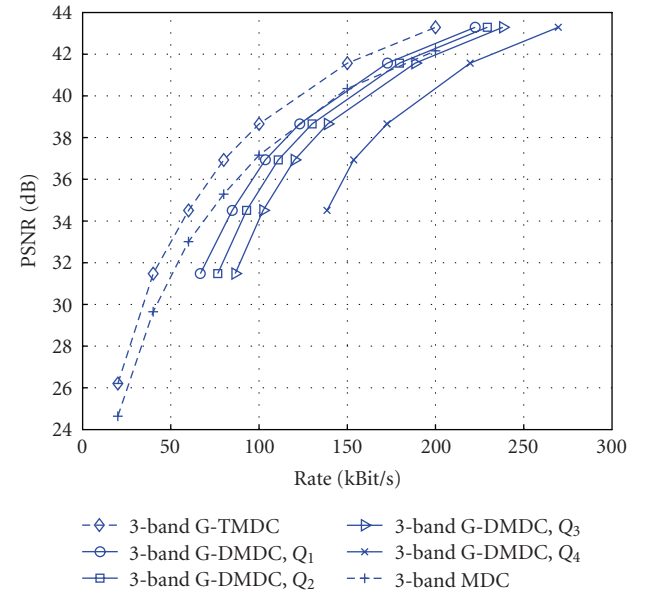


FIGURE 26: Central distortions of the 3B G-DMDC scheme compared with the 3B MDC codec (Hall Monitor, QCIF 15 fps).

use of an additional Wyner-Ziv bitstream dramatically reduces the PSNR variations with gains that could reach 100 compared to the 3-band MDC scheme at 1000 kBit/s. This figure clearly shows the benefit of using higher values of  $Q_i$  at the side decoders;  $Q_4$  being more stable than all the other schemes.

Figures 25 and 26 show the performances of the 3B G-DMDC scheme at the central decoder for Foreman and Hall Monitor. As expected, the coding performances are better than the ones with the 3B F-TMDC scheme and, this

time, the 3B G-TMDC scheme systematically outperforms the 3B MDC scheme (+1.5 dB for Foreman and +2 dB for Hall Monitor). However, the 3B G-DMDC scheme with an added WZ-encoded stream still performs worse than the 3B MDC scheme especially for the lower bitrates, and the higher  $Q_i$  is, the lower the RD performances are at the central decoder. Figures 27 and 28 show the performances of the 3B G-DMDC scheme at the side decoder. The 3B MDC scheme is outperformed even though the interpolation is done for three consecutive frames. As one can see, the 3B G-DMDC

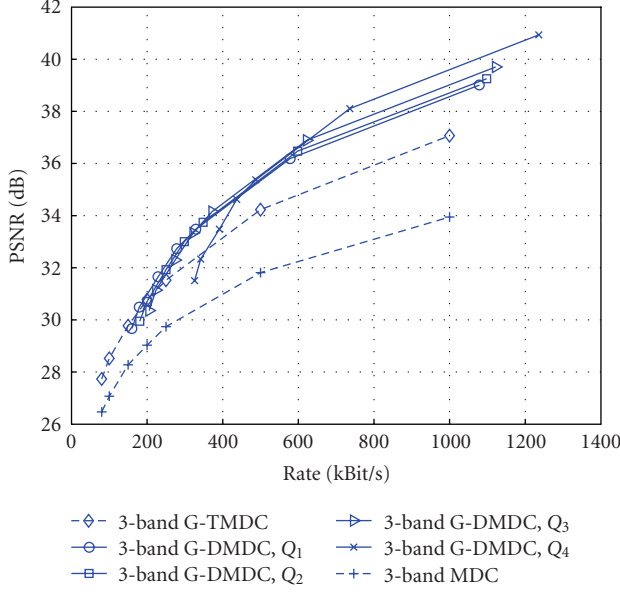


FIGURE 27: Side distortions of the 3B G-DMDC scheme compared with the 3B MDC codec (Foreman, QCIF 15 fps).

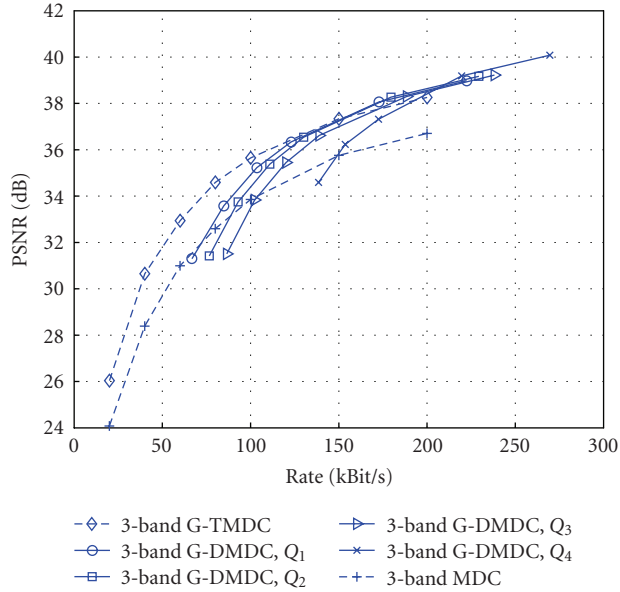


FIGURE 28: Side distortions of the 3B G-DMDC scheme compared with the 3B MDC codec (Hall Monitor, QCIF 15 fps).

scheme does not perform well compared to the 3B F-DMDC scheme because of the important amount of parity bits that are requested at the turbo decoding due to the bad quality of the SI.

Creating the two descriptions by splitting the sequence into even and odd subsequences makes the temporal filtering less efficient, the correlation between the frames is weaker and it results in poor RD performances at the central decoder. Furthermore, by sending Wyner-Ziv data for all the frames of the sequence, we end up with a totally redundant scheme. To solve this problem, we propose a 3B G-DMDC

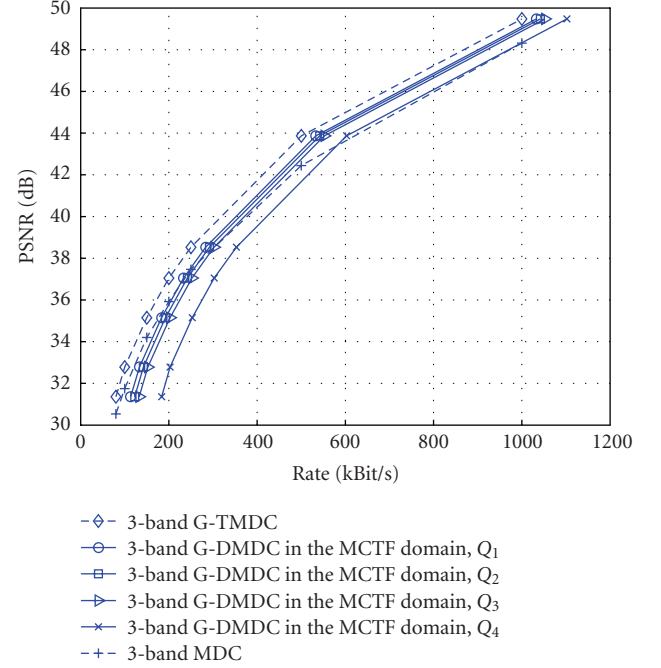


FIGURE 29: Central distortions of the 3B G-DMDC scheme in the MCTF domain compared with the 3B MDC codec (Foreman, QCIF 15 fps).

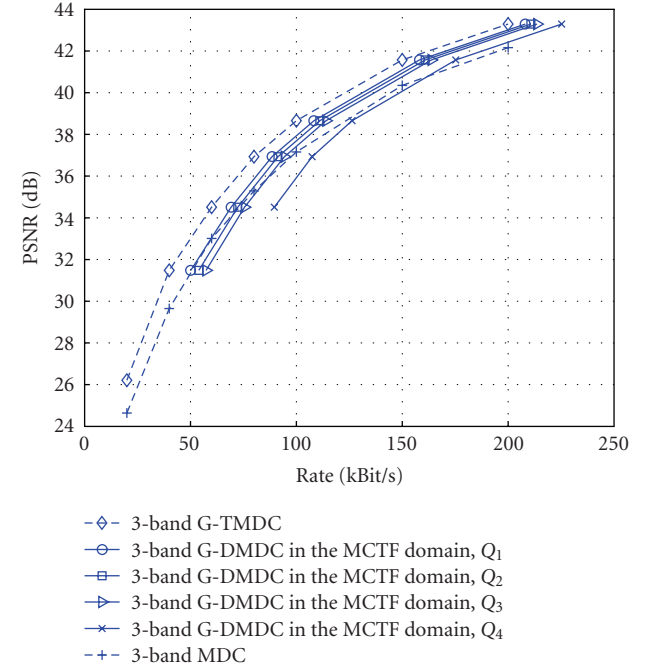


FIGURE 30: Central distortions of the 3B G-DMDC scheme in the MCTF domain compared with the 3B MDC codec (Hall Monitor, QCIF 15 fps).

scheme in the MCTF domain where the frame splitting is done as in Figure 12 and only the low-frequency subbands are WZ-encoded.

Figures 29 and 30 show the performances of the 3B G-DMDC scheme in the MCTF domain at the central decoder

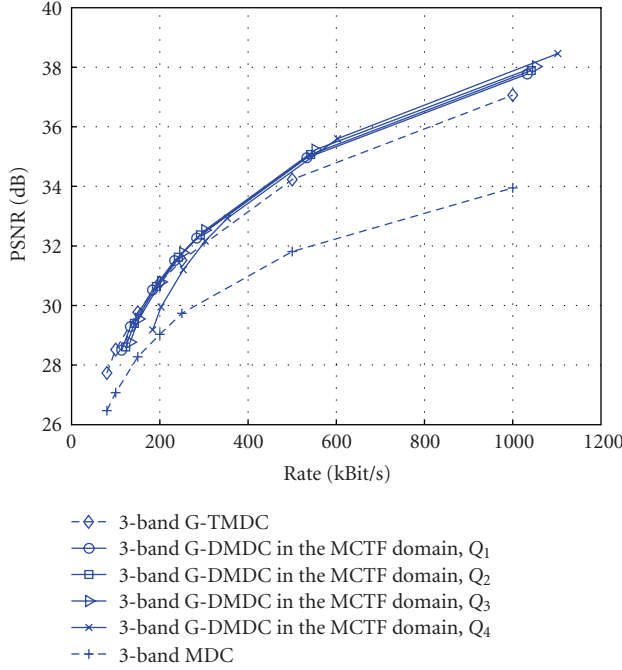


FIGURE 31: Side distortions of the 3B G-DMDC scheme in the MCTF domain compared with the 3B MDC codec (Foreman, QCIF 15 fps).

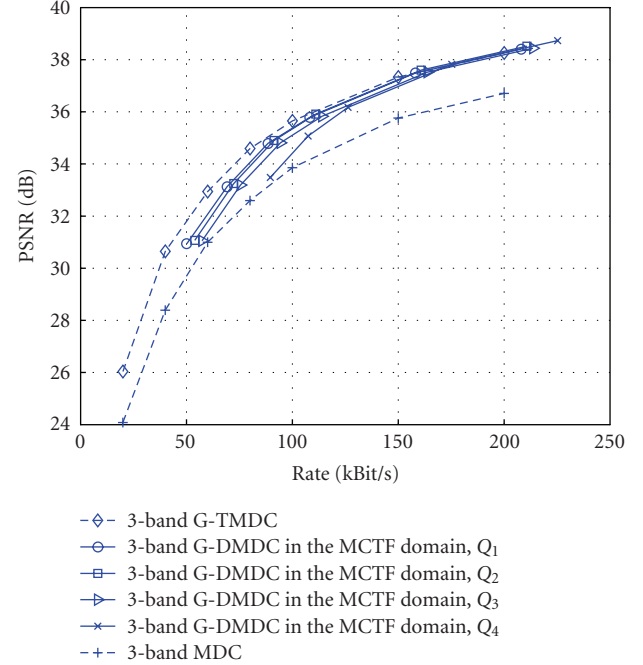


FIGURE 32: Side distortions of the 3B G-DMDC scheme in the MCTF domain compared with the 3B MDC codec (Hall Monitor, QCIF 15 fps).

for Foreman and Hall Monitor. It performs better than the 3B MDC scheme for the smallest values of  $Q_i$  ( $i < 4$ ) and the higher bitrates (starting at around 300 kBit/s for Foreman and 60 kBit/s for Hall Monitor). At the same time, the performance at the side decoder shown in Figures 31 and 32 is still better than that of the 3B MDC scheme even though it is lower than the ones of the 3B F-DMDC and 3B G-DMDC schemes.

## 7. CONCLUSION AND FUTURE WORK

In this paper, a video MDC architecture based on temporal splitting of the frames in a sequence followed by MCTF has been considered. It has first been generalized to a temporal splitting of groups of frames and to 3-band MCTF. Experimental results have shown that grouping consecutive frames before filtering and encoding them in different descriptions provides better results at the central decoder and worse results at the side decoders than directly separating even and odd frames. This effect is even more visible for high-motion sequences.

Two systematic lossy description coding schemes, where missing frames in each description are Wyner-Ziv encoded, have then been introduced in order to limit the strong quality time variations of the side descriptions of the temporal MDC approaches. The results show that both schemes perform better than the 3B MDC scheme at the side decoders for most of the bitrates and that the variation in quality between the frames is reduced, leading to less artifacts. However, the RD performances at the central decoder are always worse than that of the 3B MDC scheme even though the same schemes

without extra information perform better. This is due to the fact that, so far when used as an FEC mechanism, the Wyner-Ziv information is simply discarded when both descriptions are received and does not contribute to any improvement in the central decoding quality. Note that in presence of a return channel, the amount of WZ data can be controlled according to the impairments observed on the transmission channel. In order to have a finer tuning of the rate of the Wyner-Ziv data which has a strong impact on the tradeoff between central and side description quality, when used as an FEC mechanism, the schemes have then been extended to the case where the Wyner-Ziv frames are first temporally filtered and only the low-frequency subbands are WZ-encoded and sent as extra redundancy in the descriptions. The results showed that this scheme can outperform the 3B MDC scheme for the highest bitrates and the lowest quantization indices. The RD performance at the side decoders does not suffer too much from the fact that no Wyner-Ziv information is sent for the high-frequency subbands.

## ACKNOWLEDGMENT

The developments have been partly based on the distributed video coding software developed by the European Discover consortium which has been built upon the IST-TDWZ codec [24].

## REFERENCES

- [1] V. K. Goyal, "Multiple description coding: compression meets the network," *IEEE Signal Processing Magazine*, vol. 18, no. 5, pp. 74–93, 2001.

- [2] S. Shamaï, S. Verdú, and R. Zamir, "Systematic lossy source/channel coding," *IEEE Transactions on Information Theory*, vol. 44, no. 2, pp. 564–579, 1998.
- [3] S. Rane, A. Aaron, and B. Girod, "Systematic lossy forward error protection for error-resilient digital video broadcasting," in *Visual Communications and Image Processing (VCIP '04)*, vol. 5308 of *Proceedings of SPIE*, pp. 588–595, San Jose, Calif, USA, January 2004.
- [4] A. Sehgal, A. Jagmohan, and N. Ahuja, "Wyner-Ziv coding of video: an error-resilient compression framework," *IEEE Transactions on Multimedia*, vol. 6, no. 2, pp. 249–258, 2004.
- [5] C. Tillier and B. Pesquet-Popescu, "3D, 3-band, 3-TAP temporal lifting for scalable video coding," in *Proceedings of IEEE International Conference on Image Processing (ICIP '03)*, vol. 2, pp. 779–782, Barcelona, Spain, September 2003.
- [6] L. Ozarow, "On a source-coding problem with two channels and three receivers," *The Bell System Technical Journal*, vol. 59, no. 10, pp. 1909–1921, 1980.
- [7] A. El Gamal and T. Cover, "Achievable rates for multiple descriptions," *IEEE Transactions on Information Theory*, vol. 28, no. 6, pp. 851–857, 1982.
- [8] R. Venkataramani, G. Kramer, and V. K. Goyal, "Multiple description coding with many channels," *IEEE Transactions on Information Theory*, vol. 49, no. 9, pp. 2106–2114, 2003.
- [9] J. G. Apostolopoulos, "Reliable video communication over lossy packet networks using multiple state encoding and path diversity," in *Visual Communications and Image Processing (VCIP '01)*, B. Girod, C. A. Bouman, and E. G. Steinbach, Eds., vol. 4310 of *Proceedings of SPIE*, pp. 392–409, San Jose, Calif, USA, January 2001.
- [10] W. S. Lee, M. R. Pickering, M. R. Frater, and J. F. Arnold, "A robust codec for transmission of very low bit-rate video over channels with bursty errors," *IEEE Transactions on Circuits and Systems for Video Technology*, vol. 10, no. 8, pp. 1403–1412, 2000.
- [11] A. R. Reibman, H. Jafarkhani, Y. Wang, M. T. Orchard, and R. Puri, "Multiple-description video coding using motion-compensated temporal prediction," *IEEE Transactions on Circuits and Systems for Video Technology*, vol. 12, no. 3, pp. 193–204, 2002.
- [12] I. V. Bajic and J. W. Woods, "Domain-based multiple description coding of images and video," *IEEE Transactions on Image Processing*, vol. 12, no. 10, pp. 1211–1225, 2003.
- [13] N. Franchi, M. Fumagalli, R. Lancini, and S. Tubaro, "Multiple description video coding for scalable and robust transmission over IP," *IEEE Transactions on Circuits and Systems for Video Technology*, vol. 15, no. 3, pp. 321–334, 2005.
- [14] Y. Wang, A. R. Reibman, and S. Lin, "Multiple description coding for video delivery," *Proceedings of the IEEE*, vol. 93, no. 1, pp. 57–70, 2005.
- [15] V. A. Vaishampayan and S. John, "Balanced interframe multiple description video compression," in *Proceedings of IEEE International Conference on Image Processing (ICIP '99)*, vol. 3, pp. 812–816, Kobe, Japan, October 1999.
- [16] Y. Wang and S. Lin, "Error-resilient video coding using multiple description motion compensation," *IEEE Transactions on Circuits and Systems for Video Technology*, vol. 12, no. 6, pp. 438–452, 2002.
- [17] M. van der Schaar and D. S. Turaga, "Multiple description scalable coding using wavelet-based motion compensated temporal filtering," in *Proceedings of IEEE International Conference on Image Processing (ICIP '03)*, vol. 3, pp. 489–492, Barcelona, Spain, September 2003.
- [18] C. Tillier, B. Pesquet-Popescu, and M. van der Schaar, "Multiple descriptions scalable video coding," in *Proceedings of the 12th European Signal Processing Conference (EUSIPCO '04)*, Vienna, Austria, September 2004.
- [19] J. Kim, R. M. Mersereau, and Y. Altunbasak, "Network-adaptive video streaming using multiple description coding and path diversity," in *Proceedings of IEEE International Conference on Multimedia & Expo (ICME '03)*, vol. 2, pp. 653–656, Baltimore, Md, USA, July 2003.
- [20] N. Franchi, M. Fumagalli, G. Gatti, and R. Lancini, "A novel error-resilience scheme for a 3-D multiple description video coder," in *Proceedings of the Picture Coding Symposium*, pp. 373–376, San Francisco, Calif, USA, December 2004.
- [21] S. Cho and W. A. Pearlman, "Error resilient compression and transmission of scalable video," in *Applications of Digital Image Processing XXIII*, A. G. Tescher, Ed., vol. 4115 of *Proceedings of SPIE*, pp. 396–405, San Diego, Calif, USA, July-August 2000.
- [22] C. Tillier, B. Pesquet-Popescu, and M. van der Schaar, "Improved update operators for lifting-based motion-compensated temporal filtering," *IEEE Signal Processing Letters*, vol. 12, no. 2, pp. 146–149, 2005.
- [23] P. Chen and J. W. Woods, "Bidirectional MC-EZBC with lifting implementation," *IEEE Transactions on Circuits and Systems for Video Technology*, vol. 14, no. 10, pp. 1183–1194, 2004.
- [24] C. Brites, J. Ascenso, and F. Pereira, "Improving transform domain Wyner-Ziv video coding performance," in *Proceedings of IEEE International Conference on Acoustics, Speech, and Signal Processing (ICASSP '06)*, vol. 2, pp. 525–528, Toulouse, France, May 2006.